

Antiproliferative, Cell-Cycle Dysregulation Effects of Novel Asiatic Acid Derivatives on Human Non-small Cell Lung Cancer Cells

Liang Wang,^{a,#} Jie Xu,^{b,#} Chunhui Zhao,^{*b,d} Longxuan Zhao,^{c,d} and Bin Feng^{*a}

^aDepartment of Biotechnology, Dalian Medical University; Dalian 116044, China; ^bSchool of Life Sciences, Liaoning Normal University; ^cSchool of Chemistry and Chemical Engineering, Liaoning Normal University; Dalian 116029, China; and ^dLiaoning Provincial Key Laboratory of Biotechnology and Drug Discovery; Dalian 116029, China.

Received April 26, 2013; accepted July 23, 2013; advance publication released online August 6, 2013

Asiatic acid (AA) is a pentacyclic triterpene in *Centella asiatica* known to inhibit proliferation and induce apoptosis in several tumor cell lines. In the current study, we synthesized five AA derivatives and examined their inhibitory activities on growth in non-small cell lung cancer cell lines, A549 and PC9/G. Four derivatives were found to have stronger cell growth inhibitory activity than AA. Among them, compound A-3 showed the most significant antiproliferative effects on tumor. Growth of A549 and PC9/G cells was inhibited by A-3 in a dose- and time-dependent manner. To determine the cellular gene expression changes in A549 and PC9/G cells treated with A-3, Affymetrix GeneChip[®] Human Genome U133 Plus 2.0 Array were used to screen transcriptome differences. Expression levels of 1121 genes in A549 and 1873 genes in PC9/G were significantly altered upon treatment with 10 μ M A-3 after 48 h, with 357 overlapping genes. The signaling pathways molecules involved in the antiproliferative and cell cycle dysregulation effects of A-3 identified using microarray were further validated *via* Western blot analyses. The results collectively indicate that A-3 induces inhibition of cell proliferation *via* downregulation of the Ras/Raf/MEK/ERK pathway and cell cycle arrest at G1/S and G2/M.

Key words asiatic acid derivative; non-small cell lung cancer; microarray analysis; antiproliferation

Lung cancer, the most common cancer in terms of both incidence and mortality worldwide, was reported to have recorded 1.61 million new cases and 1.38 million deaths in 2008. Nearly 70% of all the new cases of lung cancer in the world occur in the developed countries, with the highest rates in Europe and North America.¹ Non-small cell lung cancer (NSCLC) types, including adenocarcinoma, squamous cell carcinoma and large cell carcinoma, account for more than 80% of total pulmonary malignancies.² Although drugs targeting epidermal growth factor receptor (EGFR) mutations, such as gefitinib (Iressa[®]) and erlotinib (Tarceva[®]), have been approved for treatment of advanced NSCLC, their efficacy is limited, and more than 50% of these patients are not suitable for erlotinib and gefitinib treatment.^{3,4} Furthermore, almost all patients initially sensitive to gefitinib develop resistance to the drug.^{5–7} Therefore, it is essential to identify novel anticancer drugs or reagents against NSCLC.

Asiatic acid (AA) is a pentacyclic triterpenoid derived from the tropical medicinal plant, *Centella asiatica* (Apiaceae).⁸ AA has been shown to reduce inflammation, inhibit tumor cell proliferation and induce apoptosis through a mitochondria-dependent pathway.⁹ The anti-cancer efficacy of AA is attributed to its ability to inhibit transcription factors (nuclear factor- κ B (NF- κ B)) and kinases (p38 mitogen activated protein (MAP) and extracellular signal-regulated kinase (ERK)) in a variety of tumor cells.^{9–12} AA induces apoptotic cell death in human hepatoma and malignant glioma cells through enhancing intracellular calcium release.^{13,14} The compound contains five functional groups in its structure, specifically, three hydroxyl groups at C-2, C-3, and C-23, an olefinic group at C-12, and carboxylic group at C-28, as presented in Fig. 1A. Based on previous reports that AA activities were re-

lated with the basic skeleton of pentacyclic triterpene, and the modification of C-2, C-3, C-23, and C-28 of AA can improved its biological activities.^{15,16} Dicarboxylic acid hemiesters of pentacyclic triterpenoid such as ursolic acid, oleanolic acid, and betulinic acid showed more potent inhibitory activity on human immunodeficiency virus (HIV)-protease.¹⁷ Optically active D-amino acids are widely used in the pharmaceutical industry as intermediates for the synthesis of semisynthetic antibiotics and pesticides. Among them, D-phenylglycine was used to synthesize drugs such as aspoxicillin, cefbuperazone, and cefpiramide.¹⁸ In the current study, these functional groups were modified to generate derivatives while maintaining the ursane skeleton. The carboxylic group at C-28 was converted to methyl ester with retention of stereochemistry, which may significantly influence its physical properties or receptor interactions. Butanedioic acid or D-phenylglycine was introduced into the hydroxyl group at the C-2 position, the dihydroxyl group at C-3 and C-23 was protected with acetone using 2,2-dimethoxy propane. We herein investigated the cell growth inhibition activities of AA derivatives in the human lung cancer cell lines, A549 (intermediate-sensitive)¹⁹ and PC9/G (acquired resistance to gefitinib), and clarified the mechanism of the effects.

Experimental

Reagents and Apparatus All the reagents and chemicals were of analytical grade or chemically pure, and obtained from commercial suppliers. The synthetic pathways are presented in Fig. 1B. Target compounds were purified on a silica gel column (200–300 mesh, Qingdao Marine Chemical Factory, China) with petroleum ether–ethyl acetate (or acetone) as eluents. Their structures were confirmed using nuclear magnetic resonance (NMR) on a Bruker 400MHz spectrometer (Ettlingen, Germany) and infrared radiation (IR) spectroscopy on a Shimadzu IRPrestige-21 FT-IR spectrophotometer

The authors declare no conflict of interest.

[#]These authors contributed equally to this work.

* To whom correspondence should be addressed. e-mail: binfeng70@hotmail.com; chunhuizh@hotmai.com © 2013 The Pharmaceutical Society of Japan

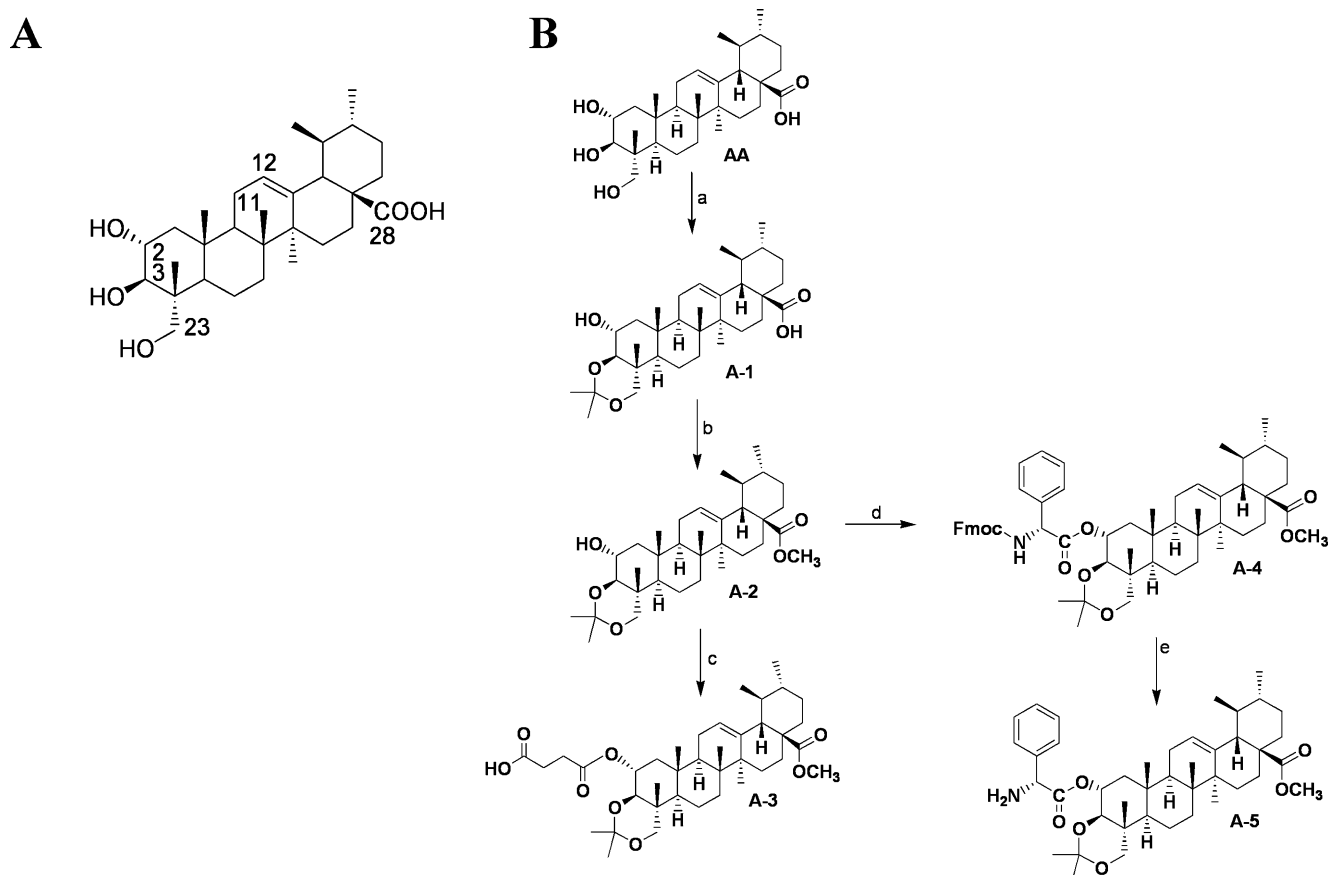


Fig. 1. Chemical Structures and Scheme

(A) Chemical structure of AA. (B) Reagents and conditions: a) $(\text{CH}_3)_2\text{C}(\text{OCH}_3)_2$, *p*-TsOH, DMF, reflux, rt; b) CH_3I , K_2CO_3 , DMF, rt; c) butanedioic anhydride, EDCI, DMAP, CH_2Cl_2 , rt; d) Fmoc-D-Phe-OH, EDCI, DMAP, CH_2Cl_2 , rt; e) HNEt_2 , CH_2Cl_2 , rt.

(Kyoto, Japan). Mass spectra were recorded on QTOF-Micro of Waters Micromass (Milford, MA, U.S.A.). Melting points were determined in capillary tubes on X-5 melting point apparatus (Beijing Tech Instrument Co., Ltd., China) and left uncorrected.

2 α , 3 β , 23-Trihydroxyurs-12-ene-28-oic Acid (AA) A solution of asiaticoside (36.34 g, 37.81 mmol) in methanol (700 mL) was added 5 M-NaOH solution (40 mL) and stirred. The reaction mixture was refluxed for overnight. After completion of the reaction by checking on the TLC (*n*-butanol–ethanol–water–ammonia water=6:4:1:0.5, v/v/v/v, disappearance of the spot $R_f=0.15$), the reaction mixture was concentrated under reduced pressure to half of its volume and neutralized with 2 M-HCl to pH 5–6. The resulting slurry was filtered and washed with large portion of water (300 mL \times 3). Filtrate was dried in drying-oven (110 $^\circ\text{C}$) to give 17 g (92%) of product as a white solid, mp 242.0–244.0 $^\circ\text{C}$. $^1\text{H-NMR}$ (400 MHz, CDCl_3) δ : 5.23 (t, 1H, $J=3.6\text{ Hz}$, H-12), 3.71–3.67 (m, 1H, H-2), 3.51 (d, 1H, $J=11.2\text{ Hz}$, H-23), 3.49 (d, 1H, $J=11.2\text{ Hz}$, H-23), 2.24 (d, 1H, $J=11.2\text{ Hz}$, H-18), 1.24, 1.03, 0.96, 0.71 (s, each 3H), 0.92 (d, 3H, $J=5.2\text{ Hz}$), 0.82 (d, 3H, $J=6.0\text{ Hz}$); $^{13}\text{C-NMR}$ (100 MHz, CDCl_3) δ : 179.81 (C-8), 140.25 (C-13), 126.71 (C-12), 78.36 (C–OH), 69.78 (C–OH), 66.32 (C–OH), 54.91, 49.56, 49.36, 49.15, 48.94, 48.72, 47.53, 44.27, 43.63, 40.65, 39.17, 38.58, 33.93, 32.28, 29.57, 25.80, 24.63, 24.30, 21.88, 19.26, 17.94, 17.85, 14.08; IR ν_{max} (KBr, cm^{-1}): 3422, 2926, 2873, 1696; electrospray ionization-mass spectra (ESI-MS):

m/z 488.0 $[\text{M}-\text{H}]^-$.

2 α -Hydroxy-3 β ,23-isopropylidenedioxyurs-12-ene-28-oic Acid (A-1) A solution of AA (15 g, 30.7 mmol) and *p*-toluenesulfonic acid (catalytic amount, 50 mg) in dry dimethyl formamide (50 mL) was added 2,2-dimethoxypropane (4.5 mL, 36.8 mmol) and stirred. The reaction mixture was stirred at room temperature for 5 h. After neutralization with 5% NaOH to pH 7–8, the reaction mixture was diluted with ethyl acetate (250 mL) and washed with water (100 mL \times 3) and saturated NaCl solution (80 mL). The organic layer was dried over anhydrous magnesium sulfate. Filtration and evaporation of solvent at reduced pressure gave light yellow solid, which was purified by silica gel chromatography with an elution of CH_2Cl_2 –MeOH (20:1, v/v) to yield a white solid (14 g, 86.2%), mp 156.4–157.8 $^\circ\text{C}$; $^1\text{H-NMR}$ (400 MHz, CDCl_3) δ : 5.24 (t, 1H, $J=3.6\text{ Hz}$, H-12), 3.80–3.76 (m, 1H, H-2), 3.50 (d, 1H, $J=10.8\text{ Hz}$, H-23), 3.46 (d, 1H, $J=10.8\text{ Hz}$, H-23), 3.32 (d, 1H, $J=9.6\text{ Hz}$, H-3), 1.45, 1.44, 1.09, 1.06, 1.04, 0.75 (s, each 3H), 0.95 (d, 3H, $J=6.0\text{ Hz}$), 0.85 (d, 3H, $J=6.5\text{ Hz}$); IR ν_{max} (KBr, cm^{-1}): 3400, 2932, 1706.

Methyl 2 α -Hydroxy-3 β ,23-isopropylidenedioxyurs-12-ene-28-oate (A-2) A solution of A-1 (16 g, 30.26 mmol) and anhydrous potassium carbonate (10.45 g, 75.64 mmol) in dry dimethyl formamide (100 mL) was added methyl iodide (3.77 mL, 60.52 mmol) and stirred. The mixture was stirred at room temperature for 6 h. The reaction mixture was diluted with ethyl acetate (500 mL) and washed with water

(200 mL×3) and saturated NaCl solution (80 mL). The organic layer was dried over anhydrous magnesium sulfate. Filtration and evaporation of solvent at reduced pressure gave light yellow solid, which was purified by silica gel chromatography with a gradient elution of ethyl acetate–petrol ether (1:4, v/v) to afford a white solid (15.1 g, 92%), mp 213.2–213.9°C; ¹H-NMR (400 MHz, CDCl₃) δ: 5.18 (t, 1H, *J*=3.6 Hz, H-12), 3.74–3.67 (m, 1H, H-2), 3.53 (s, 3H, –OCH₃), 3.44 (d, 1H, *J*=10.7 Hz, H-23), 3.39 (d, 1H, *J*=10.8 Hz, H-23), 3.25 (d, 1H, *J*=9.6 Hz, H-3), 2.53 (s, 1H, H-9), 2.17 (d, 1H, *J*=11.2 Hz, H-18), 1.38, 1.37, 1.04, 1.00, 0.97, 0.66 (s, each 3H), 0.87 (d, 3H, *J*=6.2 Hz), 0.79 (d, 3H, *J*=6.5 Hz); IR ν_{\max} (KBr, cm⁻¹): 3584, 3444, 2940, 2868, 1732.

Methyl 2 α -O-Carboxypropionyl-3 β ,23-isopropylidenedioxyurs-12-ene-28-oate (A-3) A solution of **A-2** (2.3 g, 4.24 mmol) and 4-dimethylaminopyridine (0.622 g, 5.09 mmol) in dry methylene chloride (20 mL) was added butanedioic anhydride (1.70 g, 16.96 mmol) and stirred. The mixture was refluxed for 8 h. The reaction mixture was diluted with methylene chloride (100 mL) and washed with water (50 mL×3) and saturated NaCl solution (50 mL). The organic layer was dried over anhydrous magnesium sulfate. Filtration and evaporation of solvent at reduced pressure gave light yellow solid, which was purified by silica gel chromatography with a gradient elution of ethyl acetate–petrol ether (1:4, v/v) to afford a white solid (2.49 g, 91.7%), mp 106.2–107.1°C; ¹H-NMR (400 MHz, CDCl₃) δ: 5.18 (t, 1H, *J*=3.6 Hz, H-12), 4.99–4.91 (m, 1H, H-2), 3.60 (d, 1H, *J*=10.6 Hz, H-23), 3.53 (s, 3H, –OCH₃), 3.40 (d, 1H, *J*=10.6 Hz, H-23), 2.63–2.49 (m, 4H, –CH₂CH₂–), 2.17 (d, 1H, *J*=11.4 Hz, H-18), 1.45, 1.44, 1.04, 1.02, 1.01, 0.66 (s, each 3H), 0.87 (d, 3H, *J*=6.3 Hz, H-29), 0.78 (d, *J*=6.4 Hz, H-30); ¹³C-NMR (100 MHz, CDCl₃) δ: 177.99, 176.41, 171.65, 138.18, 125.10, 99.42, 78.92, 72.67, 69.32, 52.83, 51.52, 51.13, 48.05, 47.60, 44.64, 42.06, 39.58, 39.06, 38.86, 38.35, 37.50, 36.59, 32.35, 30.64, 29.70, 29.23, 28.83, 27.98, 24.17, 23.66, 23.23, 21.20, 19.20, 17.66, 17.46, 17.01, 16.78, 13.53; IR ν_{\max} (KBr, cm⁻¹): 3320, 2942, 2570, 1710, 1449, 1382, 1180; ESI-MS: *m/z* 641.8 [M–H]⁻.

Methyl 2 α -O-(N-Fluorenonemethoxycarbonyl)-phenylglycyurs-3 β ,23-isopropylidenedioxyurs-12-ene-28-oate (A-4) A solution of **A-2** (530 mg, 0.98 mmol) and Fmoc-D-phenylglycine (550 mg, 1.46 mmol) in dry dichloromethane (8 mL) was added 4-dimethylaminopyridine (0.18 g, 1.46 mmol) and stirred. Dropwise the solution of 1-ethyl-3-(3-dimethylaminopropyl)carbodiimide hydrochloride (560 mg, 1.46 mmol) in dry dichloromethane (8 mL) to reaction mixture at 0°C. Stirring the reaction mixture for 5 min at 0°C. Keep stirring the reaction mixture for 3 h at room temperature. The reaction mixture was diluted with dichloromethane (50 mL) and washed with water (30 mL×3) and saturated NaCl solution (10 mL). The organic layer was dried over anhydrous magnesium sulfate. Filtration and evaporation of solvent at reduced pressure gave light yellow solid, which was purified by silica gel chromatography with a gradient elution of ethyl acetate–petrol ether (1:5, v/v) to afford a white solid 0.47 g, 54.03%, mp 88.2–88.5°C; ¹H-NMR (400 MHz, CDCl₃) δ: 7.69 (d, *J*=7.5 Hz, 2H, fluorenyl H-4, H-5), 7.51 (d, *J*=6.9 Hz, 2H, fluorenyl H-1', H-8'), 7.32 (d, *J*=7.4 Hz, 2H, fluorenyl H-3', H-6'), 7.26 (d, *J*=5.2 Hz, 2H, fluorenyl H-2', H-7'), 7.34–7.21 (m, 5H, Ph-H), 5.82 (d, *J*=7.2 Hz, 1H, Ph-CH), 5.26 (d, *J*=7.4 Hz, 1H, –NH), 5.18 (s, 1H, H-12), 5.10–5.08 (m, 1H, H-2), 4.34–4.30

(m, 2H, –CH₂–O), 4.15 (t, *J*=7.0 Hz, 1H, fluorenyl H-9'), 3.53 (s, 3H, –OCH₃), 3.39 (d, *J*=10.7 Hz, 1H, H-3), 3.29 (t, *J*=10.4 Hz, 2H, H-23), 2.16 (d, *J*=10.9 Hz, 1H, H-18), 1.01 (s, 9H, =C(CH₃)₂, –CH₃), 1.12, 0.92, 0.65 (each, 3H), 0.88 (d, *J*=5.3 Hz, 1H, H-29), 0.79 (d, *J*=6.5 Hz, 1H, H-30); IR ν_{\max} (KBr, cm⁻¹): 3436, 2924, 2851, 1719, 1501, 1449, 1380, 1198; ESI-MS: *m/z* 898.4 [M–H]⁻.

Methyl 2 α -O-Phenylglycyurs-3 β ,23-isopropylidenedioxyurs-12-ene-28-oate (A-5) A solution of **A-4** (420 mg, 0.47 mmol) in dry dichloromethane (8 mL) was added diethylamine (10 mL) and stirred. The reaction mixture was stirred at room temperature for 2 h. Evaporation of solvent at reduced pressure gave yellow solid, which was purified by silica gel chromatography with a gradient elution of ethyl acetate–petrol ether (1:2, v/v) to afford a white solid (0.20 g, 62%), mp 81.2–81.7°C; ¹H-NMR (400 MHz, CDCl₃) δ: 7.3–7.2 (m, 5H, Ph-H), 5.18 (t, *J*=3.5 Hz, 1H, H-12), 5.1–5.04 (m, 1H, H-2), 4.46 (s, 1H, Ph-CH), 3.53 (s, 3H, –OCH₃), 3.39 (d, *J*=10.7 Hz, 1H, H-3), 3.27 (dd, *J*₁=14.9 Hz, *J*₂=14.3 Hz, 2H, H-23), 1.01 (s, 9H, =C(CH₃)₂, –CH₃), 1.13, 0.94, 0.65 (s, each 3H), 0.88 (d, *J*=6.2 Hz, 1H, H-29), 0.79 (d, *J*=4.3 Hz, 1H, H-30); ¹³C-NMR (100 MHz, CDCl₃) δ: 177.95, 138.22, 128.52, 127.75, 127.14, 125.03, 99.18, 79.02, 76.70, 72.56, 69.22, 58.88, 52.83, 51.50, 51.02, 48.04, 47.60, 44.76, 42.05, 39.57, 39.06, 38.85, 38.38, 37.41, 36.57, 32.32, 30.64, 29.40, 27.97, 24.16, 23.63, 23.20, 21.19, 18.54, 17.70, 17.41, 16.98, 16.76, 13.52; IR ν_{\max} (KBr, cm⁻¹): 3443, 3424, 2936, 2869, 1734, 1455, 1380, 1367, 1198; ESI-MS: *m/z* 676.3 [M+H]⁺.

Cell Lines and Cultures Human NSCLC cells, A549 and PC9 were obtained from the Cell Culture Center of Chinese Academy of Medical Sciences (CAMS; Beijing, P.R. China), and maintained in RPMI 1640 (Hyclone) supplemented with 10% fetal bovine serum (FBS), penicillin (100 U/mL) and streptomycin (0.1 mg/mL). Cells were incubated at 37°C in a humidified atmosphere with 5% CO₂. Gefitinib-resistant PC9/G cells were established using a previously reported method²⁰ and treated with 0.05 μ M gefitinib (Iressa[®], ZD1839; AstraZeneca, Wilmington, DE, U.S.A.) to maintain cell resistance. A subclone of the gefitinib-resistant cell line was obtained by limited dilution, and sensitivity to gefitinib determined with Cell Counting Kit-8 (CCK-8) (Dojindo, Japan). PC9/G cells showed more than a 100-fold higher IC₅₀ for gefitinib than the parent cells.

EGFR Mutational Analysis Genomic DNA of PC9 and PC9/G cells were isolated using a MiniBEST universal genomic DNA extraction Kit (TaKaRa Biotechnology (Dalian) Co., Ltd., China). EGFR exons 19 and 20 mutation analyses were performed *via* polymerase chain reaction (PCR) using LA *Taq* DNA polymerase (TaKaRa). The primers for Exon 19 were 5'-CCA CAG GACTTT ATA ACAGGC-3' and 5'-GGC CAGTGCTGTCTCTAAGG-3', respectively. The primers for Exon 20 were 5'-CTCCCACTGCATCTGTCACTT CAC-3' and 5'-ATGCAGATGGGACAGGCACTG-3', respectively. The PCR products were analyzed by agarose gel electrophoresis and purified by MiniBEST DNA Fragment Purification Kit (TaKaRa) and sequenced (performed by TaKaRa Biotechnology).

Cell Viability Assay The proliferative activities of A549 and PC9/G cells under different treatments were assessed using the CCK-8 assay. Cells were inoculated in 96-well plates in complete medium and cultured for 24 h, and media replaced

with RPMI-1640, 10% or 1% FBS, with or without AA derivatives. All compounds were dissolved in dimethyl sulfoxide (DMSO) at final concentrations less than 0.1%, prior to addition to cell culture assays. Following incubation at 37°C for 12, 24, 48 or 72 h, 10 μ L CCK-8 was added to each well, and the plates incubated for 1–2 h. A microplate reader (Multiskan Ascen, Thermo Fisher Scientific, Waltham, MA, U.S.A.) was employed to determine optical density (OD) at 450 nm, and values compared with that of the control group. The percentage of cell viability resulting from each AA derivative was calculated as follows: $(OD_{450 \text{ treated cells}} - OD_{450 \text{ blank control}}) / (OD_{450 \text{ control}} - OD_{450 \text{ blank control}}) \times 100\%$. More than three independent experiments were performed.

Microarray Analysis Cellular RNA from A549 and PC9/G cells was extracted using TRIzol (Invitrogen), and quality controlled as directed with the Affymetrix expression technical manual. RNA (50 ng) was used to produce biotin-labeled cRNA, which was hybridized to Affymetrix GeneChip[®] Human Genome U133 Plus 2.0 Array. Array washing, scanning and probe quantification protocols were carried out according to the manufacturer's instructions using Affymetrix GeneChip Operating Software (GCOS) (<http://www.affymetrix.com>). For each array, GCOS output was imported as CEL files into Partek Genomic Suite software (Agilent), and gene expression data quantified with the RMA (Robust Multichip Averaging) algorithm, normalized and corrected for multiple testing with the Benjamini and Hochberg method for detection of differentially expressed genes.

Western Blot Analysis Total proteins were extracted from cells using RIPA buffer (Sigma). After treatment with the AA derivative, **A-3**, for 48 h, A549 and PC9/G cells were washed with ice-cold phosphate buffered saline (PBS) solution and lysed in lysis buffer at 0°C for 20 min. Cell lysates were scraped and centrifuged at 14000 rpm for 30 min at 4°C, and the supernatant collected. Equivalent amounts of proteins were subjected to sodium dodecyl sulfate-polyacrylamide gel electrophoresis (SDS-PAGE) and transferred to polyvinylidene difluoride membranes. After blocking for 1 h in 5% skimmed milk in Tris-buffered saline, the membrane was incubated with the desired primary antibody (1:2000 dilution) overnight at 4°C, followed by treatment with horseradish peroxidase-coupled secondary antibody (1:5000 dilution) for 1 h at room temperature. Immunoreactive proteins were detected using an enhanced chemiluminescence kit (Millipore, Bedford, MA, U.S.A.) and visualized using the Versa Doc Imaging System (BioRad Model 4000, CA, U.S.A.). β -Actin was used as an internal control. Antibodies used for Western blotting, specifically, EGFR, *p*-EGFR, Akt, *p*-Akt, ERK1/2, *p*-ERK1/2, mammalian target of rapamycin (mTOR), *p*-mTOR, Cyclin B, Cyclin E, CDK1, CDK2, and β -actin, were obtained from Cell Signaling Technology Inc. (Beverly, MA, U.S.A.).

Statistical Analysis All experiments were repeated three times, and data expressed as means \pm S.D. Statistical comparisons of the results were made using Student's *t*-test. The level of significance was taken at $p < 0.05$.

Results

Synthesis of AA Derivatives AA was prepared from hydrolysis of asiaticoside with 5 M NaOH in methanol, with a 90–97% yield. Using AA as the lead compound, structures were modified at C-2, C-3, C-23, and C-28. The syn-

thetic pathways are presented in Fig. 1B. AA was treated with 2,2-dimethoxypropane in the presence of *p*-toluenesulfonic acid in *N,N*-dimethylformamide (DMF) to generate acetoneide (**A-1**) with a 86.2% yield. **A-1** was subjected to methyl iodide treatment in the presence of K_2CO_3 in DMF to afford methyl ester (**A-2**) (92% yield), and **A-2** treated with butanedioic anhydride in the presence of 4-(dimethylamino)pyridine in CH_2Cl_2 to generate **A-3** (91.7% yield). **A-2** was treated with Fmoc-D-phenylglycine in the presence of 4-(dimethylamino)pyridine in CH_2Cl_2 to generate **A-4** with a 54% yield, which, in turn, was treated with diethylamine in CH_2Cl_2 to produce **A-5** with a 62% yield. Target compounds were purified on a silica gel column with petroleum ether–ethyl acetate (or acetone) as eluents and their structures confirmed using NMR and IR spectroscopy. All compounds were dissolved in DMSO at final concentrations less than 0.1%, prior to addition to cell culture assays.

Sequence of EGFR Exons 19 and 20 in PC9/G Cells Multinucleotide in-frame deletions in exon 19 that eliminate five amino acids (ELREA) are associated with increased sensitivity of lung adenocarcinomas to the selective EGFR kinase inhibitors, gefitinib (Iressa) and erlotinib (Tarceva).^{7,21} A second-site point mutation that substitutes methionine for threonine at position 790 (T790M) is associated with approximately half of case of acquired resistance to the EGFR kinase inhibitors.²¹ To determine whether PC9/G cells that acquired resistance to the gefitinib display specific genetic alterations, we analyzed the sequence of the EGFR exon 19 but found no differences in their sequences between PC9 and PC9/G cells. A deletion mutation (E746-A750), similar to that described previously,^{7,22} was identified based on alignment of sequencing data and GenBank homo sapiens genome EGFR sequence (GenBank accession number NC_000007). There is no mutation at the site in Exon 20 (position 790). The mechanism of drug resistance is thought to be multifactorial.^{20,21}

Antiproliferative Effects of AA and Its Derivatives Because cell culture medium supplemented with 10% FBS could provide the cells with an excess of growth factors overriding possible effects of drugs.²³ We treated A549 and PC9/G cell lines under normal serum conditions (10% FBS) and reduced serum conditions (1% FBS). Exposure of NSCLC to AA and its derivatives for 48 h revealed considerably higher inhibition of cell proliferation by the AA derivatives, relative to the parent compound, AA (Table 1). Under low serum conditions (1% FBS) the IC_{50} values of **A-3** (9.51 ± 4.38 , $9.73 \pm 0.11 \mu M$) and **A-5** (11.52 ± 3.58 , $13.11 \pm 2.69 \mu M$) on A549 and PC9/G cell lines were significantly lower than those of AA (44.95 ± 5.14 , $58.04 \pm 2.90 \mu M$). Under normal serum conditions (10% FBS) both A549 and PC9/G cells were significantly affected by **A-3** compared with AA, the IC_{50} values of **A-3** were 26.03 ± 2.47 and 25.57 ± 0.51 , respectively. **A-3** exerted a dose- and time-dependent antitumor effect on A549 and PC9/G, and the optimal duration of action was 48 h (Figs. 2A, B). Compounds **A-1** and **A-2** also exhibited good inhibitory activity on A549 and PC9/G cell lines in 1% FBS, the IC_{50} of **A-1** and **A-2** were $10.13 \pm 0.51 \mu M$ and $11.57 \pm 0.37 \mu M$, respectively.

A-3 Induced Gene Expression Changes in A549 and PC9/G Cells The NSCLC cell lines, A549 and PC9/G, were treated with $10 \mu M$ **A-3** for 48 h, and total RNA extracted. Microarray experiments were conducted using Affymetrix GeneChip[®] Human Genome U133 Plus 2.0 Array to deter-

Table 1. IC₅₀ Values of AA and Derivatives on A549 and PC9/G Cells Proliferation

Compounds	IC ₅₀ (μM)			
	A549		PC9/G	
	1% FBS	10% FBS	1% FBS	10% FBS
AA	44.95±5.14	>60	58.04±2.90	>60
A-1	10.13±0.51	34.73±1.74	10.58±0.63	52.45±1.31
A-2	11.57±0.37	48.86±2.93	11.02±0.66	47.61±1.67
A-3	9.51±4.38	26.03±2.47	9.73±0.11	25.57±0.51
A-4	>60	>60	>60	>60
A-5	11.52±3.58	40.21±2.01	13.11±2.69	21.66±0.97

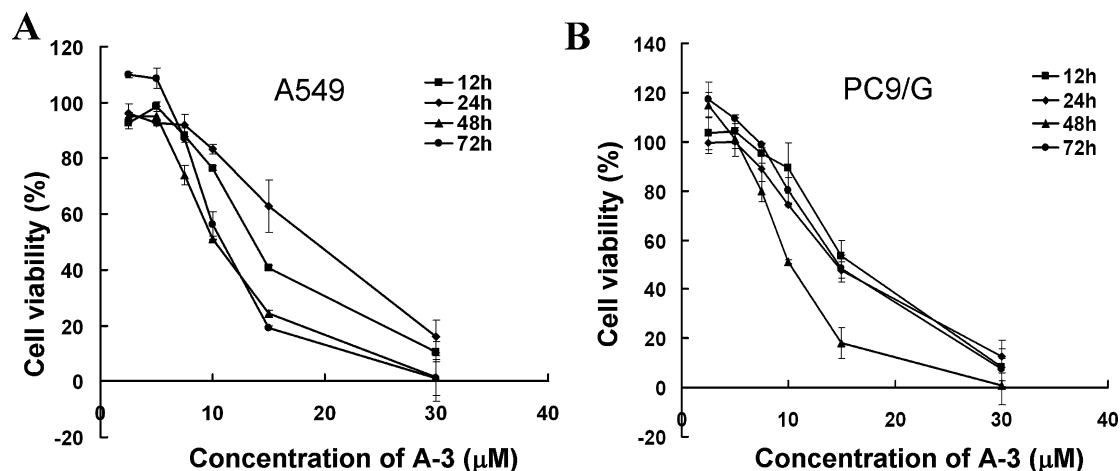


Fig. 2. Inhibitory Activities of AA and Its Derivatives on A549 and PC9/G Cell Proliferation

(A) Inhibitory activity of A-3 on A549 cells. (B) Inhibitory activity of A-3 on PC9/G cells. For (A) and (B), cells treated for the indicated times at different concentrations of A-3 were analyzed for viability with the CCK-8 assay.

mine changes in the specific genes encoding proteins related to pathological alterations in intracellular signaling pathways in response to the AA derivative, A-3. As shown in Fig. 3A, after A-3 treatment, 1121 genes in A549 cells and 1873 genes in PC9/G cells were differentially expressed, compared with controls, by at least two-fold. Venn diagram analysis facilitated the identification of a subset of 357 genes with similar functions between A549 and PC9/G cells treated with A-3 (complete list of the 357 genes is presented in Table S1).

Hierarchical clustering of the 357 genes led to segregation of A549 and PC9/G cells treated with A-3 as a separate group from control cells, according to gene expression profiles (Fig. 3B). A549 and PC9/G cells treated with A-3 clustered together, suggesting that A-3 has a transcriptomic effect on both cell types. Significant gene alterations were observed in A549 and PC9/G cells following treatment with A-3, indicating that the compound induces global changes in gene expression.

Ingenuity Pathway Analysis (IPA) of Differentially Expressed Variant Genes A gene network of 10 central nodes was constructed by using the differentially expressed genes in A549, PC9/G and controls, as described in Experimental. A dataset containing the differentially expressed genes, called the focus molecules, between NSCLC cell lines and controls was overlaid onto a global molecular network developed from information contained in the Ingenuity Pathways Knowledge Base. Networks of these focus molecules were then algorithmically generated based on their connectivity. Network mole-

cules would be found together by chance. Accordingly, a higher extent correlation indicates greater statistical significance that molecules depicted in the network are interconnected. Network contains significant deregulated genes and identified around ERK are shown in Fig. 3D. Genes are colored according to gene expression value; red gene symbols indicate up-regulation and green gene symbols indicate down-regulation. Nodes are displayed using various shapes that represent the functional class of the gene product. Dashed lines show indirect interaction, while a continuous line represents direct interactions. This result suggested that A-3 exerted its inhibition on proliferation of A549 and PC9/G through inactivation of ERK associated network, which is an important central factor in NSCLC cell growth and survival pathway.

The broad categories included genes with specific roles in cell cycle regulation, signaling and other functions as shown in Fig. 3C (the complete ingenuity pathway analysis is presented in Fig. S1). Network analysis was additionally performed to generate a graphical representation of genes with a known biological relationship. Expression levels of a number of genes in the EGFR and ERK networks were downregulated, depicted as green shading of gene icons in the network (Fig. 3D). Additional network analysis disclosed that A-3 interferes with the same pathways as the MAPK/ERK kinase-specific inhibitor, PD98059 (Fig. S2).

Effects of A-3 on Signaling Pathways and Cell Cycle Regulation Cells were treated as for microarray analysis,

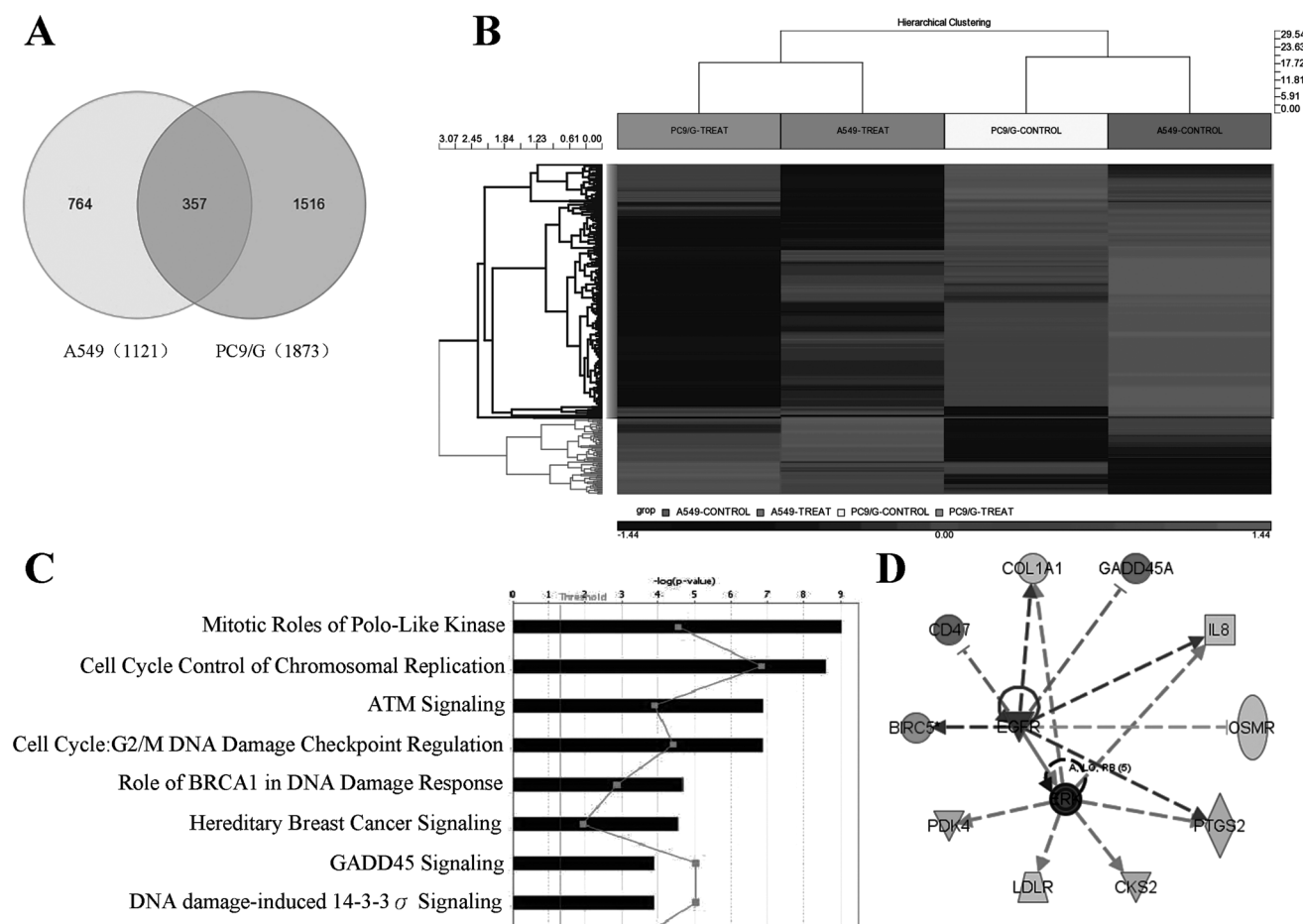


Fig. 3. Whole-Transcriptome Analysis of Cancer Cell Lines Treated with A-3

(A) Venn diagram of overlapping genes with differential expression in response to A-3. (B) Heat map of the 357 overlapping genes. Red/green indicates an increase/decrease in gene expression, relative to the universal mean for each gene. (C) Canonical pathway-based analysis of gene expression data from A549 and PC9/G cells treated with A-3. Ingenuity Pathway Analysis (IPA; Ingenuity® Systems, www.ingenuity.com) was used to identify the genes significantly associated with canonical pathways in the Ingenuity Pathways Knowledge Base. The significance of association between the significantly altered genes (fold change ≥ 2) and the canonical pathway was determined based on p values calculated with IPA statistic analysis methods. (D) EGFR and ERK signaling pathways in response to A-3 in A549 and PC9/G cells. Differential gene expression was based on treatment *versus* control expression changes (2-fold and $p < 0.05$, t -test). Red icons indicate higher expression, while green icons indicate decreased expression. Blue lines are activation functions and orange lines are inactivation. While yellow line indicates opposite result of A-3 comparing with IPA knowledge base. (Color images were converted into gray scale.)

collected, and the expression levels of phosphorylated signaling molecules analyzed *via* western blotting to examine the effects of A-3 on the EGFR downstream signaling pathway (Fig. 4A). Following treatment of cells with $10\mu\text{M}$ A-3 for 48h, EGFR phosphorylation levels of A549 and PC9/G cells were decreased, along with c-Raf and p -ERK1/2 levels, compared with their control counterparts. However, no significant variations in the phosphorylation levels of Akt and mTOR were evident in either A549 or PC9/G cell lines. Expression levels of cell cycle regulatory proteins were additionally examined *via* western blotting. Since transcriptional profiling using microarray and functional analysis revealed changes in expression levels of genes involved in cell cycle (Figs. 3C, S1), we examined the effects on cell cycle checkpoints (G1/S and G2/M) in the two cell lines after exposure to A-3. Variations in the expression levels of different kinase components were observed following A-3 treatment, including Cyclin E/CDK2 and Cyclin B/CDK1, which mainly activate cell cycle transition from G1 to S and G2 to M. As shown in Fig. 4B, A-3 induced dramatic downregulation of Cyclin E/CDK2 and Cyclin B/CDK1 in both cell lines. Our results suggest that the

kinase components of Cyclin E/CDK2 and Cyclin B/CDK1 are predominantly involved in cellular G1/S and G2/M arrest after A-3 treatment.

Discussion

Non-small cell lung cancer (NSCLC) is the leading cause of cancer-related deaths worldwide. Although a number of drugs targeting EGFR mutations have been developed to date, most advanced cases are still incurable.^{6,24,25} More than 50% of patients with NSCLC are not suitable for erlotinib and gefitinib treatment,^{3,4} and almost all patients with initial sensitivity to gefitinib develop resistance to these drugs. Novel synthetic triterpenoids mimicking physical and chemical properties of natural triterpenoids are effective in inducing apoptosis in a wide variety of tumor cells *via* diverse mechanisms and sensitizing tumor cells that do not respond to conventional chemotherapy.^{26,27}

In this study, five AA derivatives with the modification of the functional groups of C-2, C-3, C-23, and C-28 were prepared, and their antitumor activities on a gefitinib-resistant variant (PC9/G) and the gefitinib-intermediate-sensitive cell

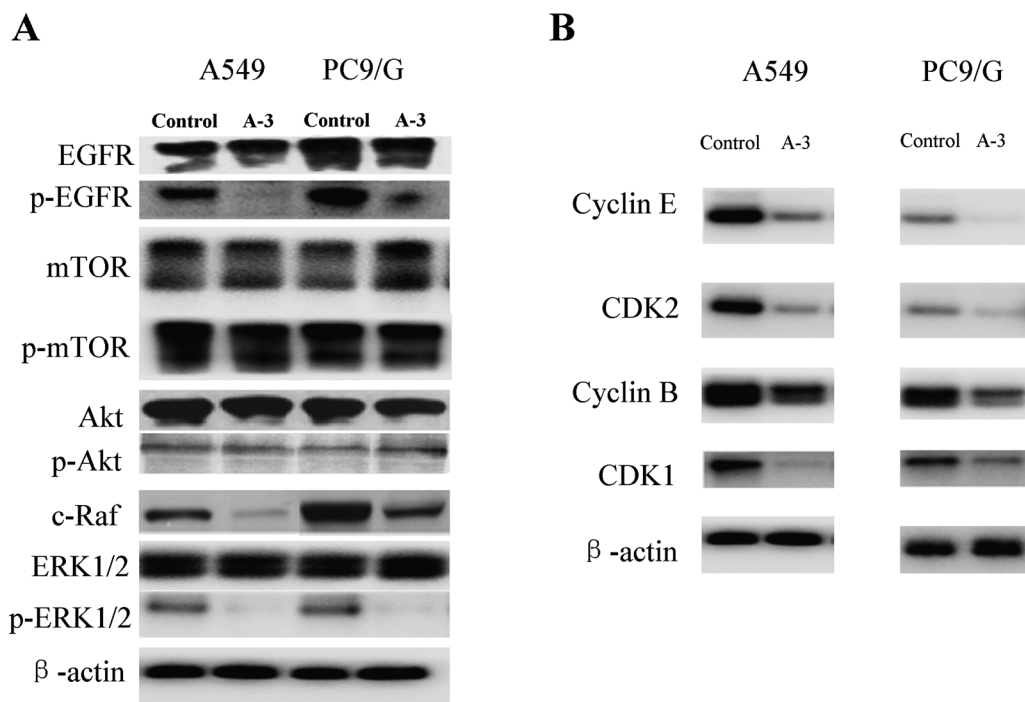


Fig. 4. Western Blot Analysis

(A) Effects of A-3 on expression levels of EGFR downstream signaling pathways in A549 and PC9/G cells. (B) Effects of A-3 on expression levels of cell cycle regulatory proteins. NSCLC cells, A549 and PC9/G, were treated with 10 μM A-3 for 48h. β-Actin was used as the loading control.

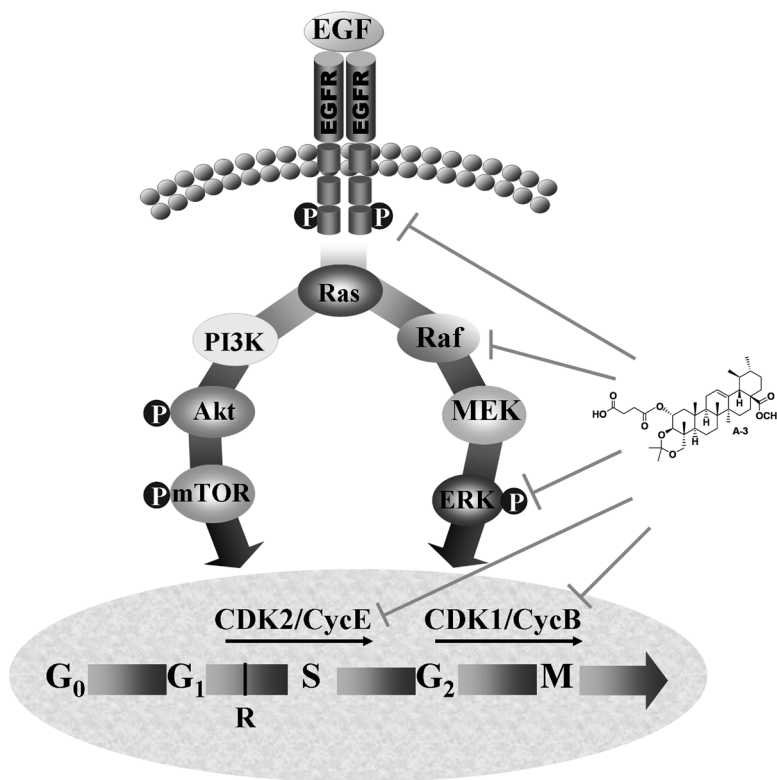


Fig. 5. Potential Mechanisms of A-3 as an Anti-tumor Agent against NSCLC Cell, A549 and PC9/G

A-3 induces inhibition of cell proliferation *via* downregulation of the Ras/Raf/MEK/ERK pathway and cell cycle arrest at G₁/S and G₂/M.

line (A549) were evaluated. Among them, compound A-3 showed the most significant antiproliferative effects on tumor cells in 10% and 1% FBS. The nearly identical cytotoxicity of compounds A-1 and A-2 suggested the unimportance of

methyl ester at C-28 for biological activity. Our data suggested that AA derivatives with cross-link at C-3 and C-23 resulted in stronger cytotoxic activities than AA against the two cell lines, and modification of AA into D-phenylglycine at C2 po-

sition increased the antitumor activity such as in compound **A-5**. However, compound **A-4** showed no activity, which might be effected by Fmoc.

A-3 displayed potent growth inhibitory activity on A549 and PC9/G cells in a concentration- and time-dependent manner. To identify transcriptome-wide gene expression changes in A549 and PC9/G cells treated with **A-3**, we performed simultaneous transcriptome analysis of cancer cell lines using Affymetrix GeneChip® Human Genome U133 Plus 2.0 Array. In total, expression changes of 1121 genes in A549 and 1873 genes in PC9/G were observed, with an overlap of 357 genes (ca. 20–30%) in both cell lines (Fig. 3A). In order to investigate the mode of action of **A-3**, we analyzed the overlapped 357 genes to evaluate the common pathway that the inhibitor (**A-3**) targeted in both of the lung cells. Genes displaying differences among **A-3**-treated cell lines, compared with control cells, were identified, and data obtained from further analyses facilitated correlation of cell growth inhibition patterns with the underlying mechanism (Fig. 3B). Ingenuity Pathway Analysis led to categorization of our data set into functional categories and networks. In A549 and PC9/G cell lines, significant alterations in genes involved in the cell cycle, particularly mitotic roles of polo-like kinase, cell cycle control of chromosomal replication, ATM signaling, and G2/M DNA damage checkpoint regulation, were observed after **A-3** treatment (Fig. 3C). Western blotting results validated significant downregulation of Cyclin E/CDK2 and Cyclin B/CDK1 by **A-3** in both cell lines and cell cycle arrest at the G1/S and G2/M transition stages (Fig. 5).

Ras/Raf/MEK/ERK and Ras/phosphatidylinositol 3-kinase (PI3K)/PTEN/Akt/mTOR signaling pathways have been shown to play key roles in the transmission of proliferative signals from membrane-bound receptors. These pathways relay extracellular information through interactions with various cellular proteins within the nucleus to control gene expression.²⁸⁾ We examined alterations in genes, focusing on the EGFR/ERK pathway identified with Ingenuity Pathway Analysis (Fig. 3D). To clarify the mechanism accounting for the effects of **A-3** on A549 and PC9/G cell lines, several key components (EGFR, p-EGFR, Akt, p-Akt, ERK1/2, p-ERK1/2, mTOR, p-mTOR, and c-Raf) of the Ras/Raf/MEK/ERK and Ras/PI3K/PTEN/Akt/mTOR signaling pathways were investigated. Expression levels of p-EGFR, p-ERK, and c-Raf were significantly downregulated in **A-3**-treated A549 and PC9/G cell lines (Fig. 4). Our results collectively suggest that the Ras/Raf/MEK/ERK pathways play important roles in the inhibition of NSCLC proliferation induced by **A-3** in A549 and PC9/G cells (Fig. 5). Future studies aimed at exploring the mechanisms of the AA derivatives in regulating tumor cell proliferation, survival, and metastasis *etc.*, will elucidate the molecular targets modulated by the AA derivatives.

In conclusion, data from the present study collectively suggest that the synthetic AA derivative, **A-3**, markedly inhibits the growth of A549 and PC9/G cells *via* downregulation of the Ras/Raf/MEK/ERK pathway and cell cycle arrest at G1/S and G2/M. Our findings support the utility of **A-3** as a potential drug in NSCLC patients.

Acknowledgment This work was jointly supported by the National Natural Science Foundation of China (No. 21102067, No. 81071248).

References

- 1) Ferlay J., Shin H. R., Bray F., Forman D., Mathers C., Parkin D. M., *Int. J. Cancer*, **127**, 2893–2917 (2010).
- 2) Zalcman G., Bergot E., Lechapt E., *Eur. Respir. Rev.*, **19**, 173–185 (2010).
- 3) Sharma S. V., Bell D. W., Settleman J., Haber D. A., *Nat. Rev. Cancer*, **7**, 169–181 (2007).
- 4) Ciardiello F., Tortora G., *N. Engl. J. Med.*, **358**, 1160–1174 (2008).
- 5) Qi H. W., Shen Z., Fan L. H., *Exp. Ther. Med.*, **2**, 1091–1095 (2011).
- 6) Cappuzzo F., Hirsch F. R., Rossi E., Bartolini S., Ceresoli G. L., Bemis L., Haney J., Witta S., Danenberg K., Domenichini I., Ludovini V., Magrini E., Gregorc V., Doglioni C., Sidoni A., Tonato M., Franklin W. A., Crino L., Bunn P. A. Jr., Varella-Garcia M., *J. Natl. Cancer Inst.*, **97**, 643–655 (2005).
- 7) Lynch T. J., Bell D. W., Sordella R., Gurubhagavatula S., Okimoto R. A., Brannigan B. W., Harris P. L., Haserlat S. M., Supko J. G., Haluska F. G., Louis D. N., Christiani D. C., Settleman J., Haber D. A., *N. Engl. J. Med.*, **350**, 2129–2139 (2004).
- 8) James J. T., Dubery I. A., *Molecules*, **14**, 3922–3941 (2009).
- 9) Tang X. L., Yang X. Y., Jung H. J., Kim S. Y., Jung S. Y., Choi D. Y., Park W. C., Park H., *Biol. Pharm. Bull.*, **32**, 1399–1405 (2009).
- 10) Hsu Y. L., Kuo P. L., Lin L. T., Lin C. C., *J. Pharmacol. Exp. Ther.*, **313**, 333–344 (2005).
- 11) Gurfinkel D. M., Chow S., Hurren R., Gronda M., Henderson C., Berube C., Hedley D. W., Schimmer A. D., *Apoptosis*, **11**, 1463–1471 (2006).
- 12) Park B. C., Bosire K. O., Lee E. S., Lee Y. S., Kim J. A., *Cancer Lett.*, **218**, 81–90 (2005).
- 13) Lee Y. S., Jin D. Q., Kwon E. J., Park S. H., Lee E. S., Jeong T. C., Nam D. H., Huh K., Kim J. A., *Cancer Lett.*, **186**, 83–91 (2002).
- 14) Cho C. W., Choi D. S., Cardone M. H., Kim C. W., Sinskey A. J., Rha C., *Cell Biol. Toxicol.*, **22**, 393–408 (2006).
- 15) Zhao L. X., Tian M. Z., Jin L. J., He X. L., Shen P., Zhang X. C., Yang J. W., *Chinese J. Org. Chem.*, **31**, 646–652 (2011).
- 16) Zhao L. X., Park H. G., Jew S. S., Lee M. K., Kim Y. C., Thapa P., Karki R., Jahng Y., Jeong B. S., Lee E. S., *Bull. Korean Chem. Soc.*, **28**, 970–976 (2007).
- 17) Ma C., Nakamura N., Miyashiro H., Hattori M., Shimotohno K., *Chem. Pharm. Bull.*, **47**, 141–145 (1999).
- 18) Takenaka S., Honma Y., Yoshida K., Yoshida K., *Biotechnol. Lett.*, **35**, 1053–1059 (2013).
- 19) Noro R., Gemma A., Kosaihiira S., Kokubo Y., Chen M., Seike M., Kataoka K., Matsuda K., Okano T., Minegishi Y., Yoshimura A., Kudoh S., *BMC Cancer*, **6**, 277 (2006).
- 20) Koizumi F., Shimoyama T., Taguchi F., Saijo N., Nishio K., *Int. J. Cancer*, **116**, 36–44 (2005).
- 21) Bean J., Brennan C., Shih J. Y., Riely G., Viale A., Wang L., Chitale D., Motoi N., Szoke J., Broderick S., Balak M., Chang W. C., Yu C. J., Gazdar A., Pass H., Rusch V., Gerald W., Huang S. F., Yang P. C., Miller V., Ladanyi M., Yang C. H., Pao W., *Proc. Natl. Acad. Sci. U.S.A.*, **104**, 20932–20937 (2007).
- 22) Paez J. G., Janne P. A., Lee J. C., Tracy S., Greulich H., Gabriel S., Herman P., Kaye F. J., Lindeman N., Boggon T. J., Naoki K., Sasaki H., Fujii Y., Eck M. J., Sellers W. R., Johnson B. E., Meyerson M., *Science*, **304**, 1497–1500 (2004).
- 23) Warburton C., Dragowska W. H., Gelmon K., Chia S., Yan H., Masin D., Denyssevych T., Wallis A. E., Bally M. B., *Clin. Cancer Res.*, **10**, 2512–2524 (2004).
- 24) Pao W., Miller V., Zakowski M., Doherty J., Politi K., Sarkaria I., Singh B., Heelan R., Rusch V., Fulton L., Mardis E., Kupfer D., Wilson R., Kris M., Varmus H., *Proc. Natl. Acad. Sci. U.S.A.*, **101**, 13306–13311 (2004).
- 25) Bell D. W., Lynch T. J., Haserlat S. M., Harris P. L., Okimoto R. A., Brannigan B. W., Sgroi D. C., Muir B., Riemenschneider M. J., Iacona R. B., Krebs A. D., Johnson D. H., Giaccone G., Herbst R. S., Manegold C., Fukuoka M., Kris M. G., Baselga J., Ochs J. S., Haber

- D. A., *J. Clin. Oncol.*, **23**, 8081–8092 (2005).
- 26) Shanmugam M. K., Nguyen A. H., Kumar A. P., Tan B. K., Sethi G., *Cancer Lett.*, **320**, 158–170 (2012).
- 27) Hyer M. L., Croxton R., Krajewska M., Krajewski S., Kress C. L., Lu M., Suh N., Sporn M. B., Cryns V. L., Zapata J. M., Reed J. C., *Cancer Res.*, **65**, 4799–4808 (2005).
- 28) Steelman L. S., Chappell W. H., Abrams S. L., Kempf R. C., Long J., Laidler P., Mijatovic S., Maksimovic-Ivanic D., Stivala F., Mazarino M. C., Donia M., Fagone P., Malaponte G., Nicoletti F., Libra M., Milella M., Tafuri A., Bonati A., Bäsecke J., Cocco L., Evangelisti C., Martelli A. M., Montalto G., Cervello M., McCubrey J. A., *Aging* (Albany, NY), **3**, 192–222 (2011).